METAS

GNSS stations relative calibration

G1/G2 #1013-2024

Michel Abgrall, Baptiste Chupin

Observatoire de Paris

michel.abgrall@obspm.fr, baptiste.chupin@obspm.fr, caroline.lim@obspm.fr

June 21, 2024
Issue 1.0

1 Introduction.

1.1 General informations.

This calibration report released by LNE-SYRTE is about the G1/G2 relative calibration campaign of GNSS stations located in METAS. This campaign took place from 19 February 2024 (MJD 60359) to 20 April 2024 (MJD 60420).
The report is built according to the Annex 4 of the document "BIPM guidelines for GNSS calibration" [1] and contains all the required informations, data, plots and results either required by BIPM in the frame of the CCTF Working Group on GNSS, or by BIPM and EURAMET in the frame of the Group1/Group2 calibration scheme. It also contains the uncertainty budget computation according to the Guidelines, which is showing whether the calibrated links used in the frame of the TAI computation would be in line with the conventional values.
This report is consistent with the capabilities that are included in Appendix C of the CIPM MRA drawn up by the CIPM. Under the CIPM MRA, all participating institutes recognize the validity of each other's calibration and measurement certificates for the quantities, ranges and measurement uncertainties specified in the KCDB (for details see `https://www.bipm.org/kcdb/`).
The first section of this document gives the introduction, the document structure, the list of acronyms and of the reference documents. Section 2 contains a summary of the results. Section 3 describes the equipment and operations during the calibration campaign. Section 4 provides all informations about data handling and calibration processing. Section 5 is about the calibration results between stations, and Section 6 is devoted to the uncertainty budgets computation. This document finish with an assessment of the stability of the GNSS reference station and of the traveling ones during this campaign in Section 7.
Annex A provides the required BIPM information sheets for all GNSS stations involved, Annex B shows the plots of the raw data together with the related TDEV. Annex C describes all the terms appearing in the uncertainty budgets.

1.2 Calibration report changes.

This is Issue 1.0 of the calibration report

1.3 Acronym list.

ADEV:	Allan deviation, square root of AVAR
AVAR:	Allan variance or Two-sample variance
BIPM:	Bureau International des Poids et Mesures
CCTF:	Consultative Committee on Time and Frequency
CGGTTS:	CCTF Global GNSS Time Transfer Standard format
CIPM:	Comité International des Poids et Mesures
CV:	Common-view
Galileo:	European Union GNSS
GFZ:	Geoforschungszentrum, Germany
GLONASS:	Russian GNSS
GNSS:	Global Navigation Satellite System
GPS:	United States of America GNSS
IGS:	International GNSS Service
LNE:	Laboratoire National de Métrologie et d'Essais, France
LNE-SYRTE:	French designated laboratory in charge of time and frequency units
MDEV:	Modified Allan deviation, square root of MVAR
MVAR:	Modified Allan variance
NA:	Not Applicable
NMI:	National Metrology Institute
NRCan:	National Resources Canada
OP:	Observatoire de Paris, France
PPP:	Precise Point Positioning
PPS:	Pulse per second
RINEX:	Receiver international exchange format for Geodesy
SYRTE:	Systèmes de Référence Temps-espace, OP laboratory where LNE-SYRTE is located
TDEV:	Time Allan deviation, square root of TVAR
TIC:	Time Interval Counter
TVAR:	Time Allan variance

1.4 Reference documents.

[1] BIPM. *"BIPM guidelines for GNSS calibration"*. Version V4.0. 05/08/2021.

[2] G. D. Rovera, M. Abgrall, P. Uhrich, P. Defraigne, and B. Bertrand. "GNSS antenna multipath effects". In: *Proc. of the 31st European Frequency and time Forum (EFTF)*. Torino, Italy, 2018.

[3] G. D. Rovera, M. Siccardi, S. Römisch, and M. Abgrall. "Time delay measurements: estimation of the error budget". In: *Metrologia* 56.3 (2019).

[4] G. D. Rovera, M. Abgrall, P. Uhrich, and M. Siccardi. "Techniques of antenna cable delay measurement for GPS time transfer". In: *Proc. of the 5th International Colloquium on Scientific and Fundamental Aspects of the Galileo Programme*. Braunschweig, Germany, 27-29 October 2015.

[5] P. Uhrich and D. Valat. "GPS receiver relative calibration campaign preparation for Galileo In-Orbit Validation". In: *Proc. of the 24th European Frequency and time Forum (EFTF)*. Noordwijk, The Netherlands, April 2010.

[6] G. D. Rovera, J.-M. Torre, R. Sherwood, M. Abgrall, C. Courde, M. Laas-Bourez, and P. Uhrich. "Link calibration against receiver calibration: an assessment of GPS time transfer uncertainties". In: *Metrologia* 51.5 (2014), pp. 476–490.

2 Summary of the results.

This Section is a summary of the station relative calibration results. Table 1 provides the GPS P1-code and P2-code calibrated delays for METAS stations, from where the ionosphere-free linear combination P3 delays are computed, together with their related uncertainties according to the conventional values. Table 2 provides the GALILEO E1-code and E5a-code calibrated delays and the ionosphere-free linear combination E3 computed delay, together with the related uncertainties according to the conventional values. These results are fully valid for the period of the calibration campaign. The results for each code are in agreement to better than 1 ns with respect to the previous calibration of METAS stations performed by PTB and METAS, which access the stability of METAS stations together with OP reference station.

Table 1: Summary of the stations GPS delays (all values in ns)

Station	Measure-ment period	P1 delays	Combined uncertainty	P2 delays	Combined uncertainty	P3 delays	Combined uncertainty	Combined uncertainty [*]
CH04	60385–60392	28.268	0.7	24.918	0.7	33.446	0.8	2.5
CH05	60385–60392	26.080	0.7	23.916	0.7	29.425	0.8	2.5

[*] Conventional combined uncertainty value for G1/G2 calibration, including the OP reference station combined uncertainty.

Table 2: Summary of the stations GALILEO delays (all values in ns)

Station	Measure-ment period	E1 delays	Combined uncertainty	E5a delays	Combined uncertainty	E3 delays	Combined uncertainty	Combined uncertainty [*]
CH04	60385–60392	30.676	0.7	29.634	0.7	31.990	0.7	2.5
CH05	60385–60392	28.477	0.7	26.852	0.7	30.525	0.7	2.5

[*] Conventional combined uncertainty value for G1/G2 calibration, including the OP reference station combined uncertainty.

3 Description of equipment.

3.1 OP GNSS equipment.

OP73 is currently made of a Septentrio multichannel multi-GNSS PolaRx5-TR, a high quality 30 m antenna cable and a SepChoke B3/E6 multi-GNSS choke-ring antenna. This station was part of the last G1 calibration campaign (# 1001-2022), its delays having been computed by BIPM with P3 and E3 time transfer conventional combined uncertainties of 1.8 ns for GPS and 1.5 ns GALILEO, respectively.
The OP GNSS traveling equipment is made of two multi-GNSS Septentrio PolaRx5-TR main units called OP72 and OP74, connected to one single 70 m long antenna cable thanks to a power splitter, and to one single multi-GNSS Veraphase 6000 antenna.
All the OP PolaRx5-TR receivers involved in this calibration are operated with the PPS-In delay compensation disabled: the PPS-Out connectors define their reference point for refdelay measurements.

3.2 METAS GNSS equipment.

The METAS GNSS equipment to calibrate was based on two Septentrio PolaRx5-TR main units both connected to their own SepChoke B3/E6 multi-GNSS choke-ring antenna via antenna cables. Both METAS receivers are operated with the PPS-In delay compensation ensabled: the PPS-In connectors define their reference point for refdelay measurements. Annex A contains the details about the local implementations in the visited stations. These stations were calibrated as G2 GNSS stations according to the BIPM Guidelines for the delays computations including the related combined uncertainties.

3.3 Summary of the involved equipment and planning.

Table 3 summarizes the equipment involved in the GNSS relative calibration campaign with highlighted traveling station measurement periods on each site.

Table 3: Description of equipment

Institute	Status of equipement	MJD of measurement	Receiver type	BIPM code	RINEX name
OP	Traveling		Septentrio PolaRx5TR	OP72	OP7200FRA
OP	Traveling		Septentrio PolaRx5TR	OP74	OP7400FRA
OP	Groupe 1 Reference	60359 – 60366	Septentrio PolaRx5TR	OP73	OP7300FRA
OP	Groupe 1 Reference	60413 – 60420	Septentrio PolaRx5TR	OP73	OP7300FRA
METAS	Groupe 2	60385 – 60392	Septentrio PolaRx5TR	CH04	WAB200CHE
METAS	Groupe 2	60385 – 60392	Septentrio PolaRx5TR	CH05	ch0500CHE

4 Data and processing.

All OP collected raw Septentrio binary files (SBF) data are transformed into GNSS RINEX 3 format by using the Septentrio proprietary SBF2RIN software. Local receivers SBF and/or RINEX 3 and/or RINEX 2 data, together with CGGTTS files when they exist, are provided by the visited institution/laboratory. The calibration is consisting in building differential 30 s sampled CGGTTS data for each P1- and P2- codes for GPS and for each E1- and E5a- codes for Galileo between pairs of receivers, for which we partly use the R2CGGTTS software developed by P. Defraigne (ORB). Another part of the calibration software is an original development by LNE-SYRTE. These CGGTTS differences are corrected by the known reference delay (REFDLY) and antenna cable delay (CABDLY) when available. In this case, the calibrated delays are for the ensemble receiver main unit plus antenna.
For each location, the coordinates of the antenna phase centers are especially computed for the calibration period from RINEX 2 files by using the NRCan PPP software. Unfortunately, this computation is limited to GPS phase center for L1 and L2 carrier frequencies. Galileo E1 carrier being equal to L1, we assume the phase center is identical. But it is not the case for Galileo E5a compared to L2, and we can only approximate the Galileo E5a phase center by using L2 one. The geometric correction between pairs of antenna phase centers for receivers in common-clock set-up is computed by using Rapid BRDC files provided by IGS.
Reference delays are measured against either the local UTC(k) physical reference point or the local time scale reference point at the trigger level currently used in the involved laboratories. The trigger level in LNE-SYRTE is 1.0 V. Antenna cable delay is either obtained from dedicated measurements or included in the P1 and P2 delays and in the E1 and E5a delays when no value is available for this parameter. In this latter case, the CABDLY value is set to 0 in the parameter file, and the calibrated delays are for the ensemble receiver main unit plus antenna cable plus antenna.
For validation purposes, ionosphere-free linear combinations P3 and E3 CGGTTS files are computed by using the R2CGGTTS software provided by P. Defraigne (ORB), and CV are built between pairs of receivers. This is more especially the case when we are using two traveling receivers in a visited location, in order to better assess the stability of this traveling ensemble all over the calibration campaign. The conservative estimated value for the traveling equipment stability during such a campaign is typically chosen for each code as the maximum between the misclosure between the start and the end of the campaign and the average offset between both traveling receivers as measured in each location.
As conservative estimate, the noise of the P1 and P2 differences and of the E1 and E5a differences is obtained from the highest value of the one-sigma statistical uncertainty of the TDEV at 1 d, issued from a linear interpolation between consecutive TDEV points when required. In the case there is not enough data to compute a TDEV at 1 d, the upper limit of the last error bar available is considered as noise of the raw differences. The noise of P3 and E3 data is issued from a similar analysis on TDEV data.

5 Results of raw data processing.

Table 4 and table 5 provide a summary of all the delays involved in the GPS code and in the GALILEO code, respectively. The tables provide first the calibration of the traveling stations OP72 and OP74 against the reference station OP73 at the start and the end of the campaign, from which we estimate, from an average, the internal delays to be accounted for during measurements at the remote site. Then the tables show the calibration of the visited stations against these traveling receivers. The calibration results summarized in tables 1 and 2 are computed from the average delays of both traveling receivers. The misclosure remains below 400 ps for each GPS and GALILEO codes. As typically expected, the noise estimates from the TDEVs are below 100 ps, and are hence remaining low enough in the uncertainty budgets (see Section 6). All the plots of P1, P2, E1 and E5a differences are provided in Annex B, together with the related TDEV analysis. The P3 and E3 computed by using the results of the calibration and the related TDEV are also made available in Annex B.

Table 4: Summary of **GPS** delays

Receiver	Reference	MJD of Measurement	REFDLY	CABDLY	P1 DLY	TDEV	P2 DLY	TDEV	P3 DLY	TDEV
OP73	Ref	60359 – 60366	85.2	129.6	29.550	NA	26.020	NA	35.006	NA
OP72	OP73	60359 – 60366	93.4	0.0	299.501	0.027	297.345	0.031	302.834	0.094
OP74	OP73	60359 – 60366	111.4	0.0	300.153	0.026	298.068	0.031	303.376	0.092
OP73	Ref	60413 – 60420	85.2	129.6	29.550	NA	26.020	NA	35.006	NA
OP72	OP73	60413 – 60420	93.3	0.0	299.127	0.026	297.045	0.025	302.345	0.093
OP74	OP73	60413 – 60420	111.3	0.0	299.794	0.026	297.774	0.025	302.916	0.090
OP72	Ref	60385 – 60392	45.2	0.0	299.315	NA	297.195	NA	302.592	NA
CH04	OP72	60385 – 60392	2.5	208.9	28.266	0.035	24.921	0.047	33.436	0.137
CH05	OP72	60385 – 60392	9.2	220.0	26.078	0.027	23.919	0.046	29.415	0.120
OP74	Ref	60385 – 60392	63.8	0.0	299.975	NA	297.920	NA	303.151	NA
CH04	OP74	60385 – 60392	2.5	208.9	28.270	0.035	24.915	0.048	33.456	0.142
CH05	OP74	60385 – 60392	9.2	220.0	26.081	0.027	23.913	0.046	29.432	0.123

Table 5: Summary of **Galileo** delays

Receiver	Reference	MJD of Measurement	REFDLY	CABDLY	E1 DLY	TDEV	E5a DLY	TDEV	E3 DLY	TDEV
OP73	Ref	60359 – 60366	85.2	129.6	31.780	NA	31.520	NA	32.108	NA
OP72	OP73	60359 – 60366	93.4	0.0	301.838	0.026	301.315	0.047	302.497	0.064
OP74	OP73	60359 – 60366	111.4	0.0	302.635	0.027	302.037	0.049	303.389	0.067
OP73	Ref	60413 – 60420	85.2	129.6	31.780	NA	31.520	NA	32.108	NA
OP72	OP73	60413 – 60420	93.3	0.0	301.472	0.026	300.970	0.030	302.105	0.065
OP74	OP73	60413 – 60420	111.3	0.0	302.281	0.026	301.706	0.030	303.006	0.065
OP72	Ref	60385 – 60392	45.2	0.0	301.655	NA	301.142	NA	302.302	NA
CH04	OP72	60385 – 60392	2.5	208.9	30.674	0.027	29.636	0.043	31.983	0.069
CH05	OP72	60385 – 60392	9.2	220.0	28.475	0.042	26.853	0.044	30.520	0.107
OP74	Ref	60385 – 60392	63.8	0.0	302.457	NA	301.872	NA	303.194	NA
CH04	OP74	60385 – 60392	2.5	208.9	30.679	0.028	29.633	0.043	31.998	0.070
CH05	OP74	60385 – 60392	9.2	220.0	28.479	0.042	26.850	0.044	30.533	0.106

6 Uncertainty budgets.

Tables 6, 7, 8, 9 are providing the uncertainty budget for the computed internal delays of the METAS CH4 and CH5 stations for GPS and for GALILEO, respectively. See Annex C for detailed explanations about the different terms.
The Type A uncertainty on measured codes is estimated from the high value of the 1 sigma statistical uncertainty of the TDEV(1 d). To be conservative, we take the largest value obtained within the two traveling receivers. The Type A uncertainty of the difference between codes is the quadratic sum between both estimations. The P3 and E3 Type A uncertainties are estimated from the high value of the 1 sigma statistical uncertainty of the related TDEV(1 d). All TDEV plots are in Annex B.
In the calibration process only P1 and P2 delays for GPS and E1 and E5a delays for Galileo are estimated, therefore the misclosure for P3 delay (GPS) or E3 delay (Galileo) is not directly available from the calibration computation. The GPS P3 misclosure is estimated by applying to the misclosure values computed for P1- and P2- code the ionosphere-free linear combination formula:
P3 = P1 + 1.546 x (P1 - P2)
The Galileo E3 misclosure is estimated by applying to the misclosure values computed for E1- and E5a- code the ionosphere-free linear combination formula:
E3 = E1 + 1.261 x (E1 - E5a)
It was not necessary to measure separately the antenna cable delays (CABDLY) of the traveling equipment which remained in the same configuration at OP and at the visited site. Therefore the corresponding uncertainties are expected to be negligible.

Table 6: **CH04** uncertainty budget for **GPS** calibrated delays

Uncertainty type	P1	P2	P1-P2	P3	Description
u_a(Reference)	0.027	0.031	0.041	0.094	Largest TDEV(1 d) sigma between the start and the end of OP72 or OP74 against OP73
u_a(CH04)	0.035	0.047	0.059	0.142	Largest TDEV(1 d) sigma of offset between visited station and OP72 or OP74
Type A uncertainties					
u_a	0.044	0.057	0.073	0.170	Visited against reference
Misclosure					
$u_{b,1}$	0.367	0.298	0.070	0.474	Actual misclosure offset
Systematic components related to RAWDIF					
$u_{b,11}$	0.200	0.200	0.200	0.200	Position error at OP
$u_{b,12}$	0.200	0.200	0.200	0.200	Position error at visited site
$u_{b,13}$	0.200	0.200	0.200	0.200	Multipaths at OP
$u_{b,14}$	0.200	0.200	0.200	0.200	Multipaths at visited site
Link of the traveling system to local time scale					
$u_{b,21}$	0.220	0.220		0.220	REFDLY at OP
$u_{b,22}$	0.220	0.220		0.220	REFDLY at visited site
$u_{b,TOT}$	0.626	0.588	0.407	0.694	
Link of the reference system to UTC(OP)					
$u_{b,31}$	0.220	0.220		0.220	REFDLY at OP
Link of the visited system to its local time scale					
$u_{b,32}$	0.220	0.220		0.220	REFDLY at visited site
Antenna cable delays					
$u_{b,41}$	0.000	0.000		0.000	CABDLY at OP
$u_{b,42}$	0.000	0.000		0.000	CABDLY at visited site
Type B uncertainties					
$u_{b,SYS}$	0.700	0.666		0.761	Quadratic sum of u_b
Combined uncertainties					
u_{CAL0}	0.702	0.669		0.780	Composed of u_a and $u_{b,SYS}$

Table 7: **CH05** uncertainty budget for **GPS** calibrated delays

Uncertainty type	P1	P2	P1-P2	P3	Description
u_a(Reference)	0.027	0.031	0.041	0.094	Largest TDEV(1 d) sigma between the start and the end of OP72 or OP74 against OP73
u_a(CH05)	0.027	0.046	0.053	0.122	Largest TDEV(1 d) sigma of offset between visited station and OP72 or OP74
Type A uncertainties					
u_a	0.038	0.056	0.068	0.155	Visited against reference
Misclosure					
$u_{b,1}$	0.367	0.298	0.070	0.474	Actual misclosure offset
Systematic components related to RAWDIF					
$u_{b,11}$	0.200	0.200	0.200	0.200	Position error at OP
$u_{b,12}$	0.200	0.200	0.200	0.200	Position error at visited site
$u_{b,13}$	0.200	0.200	0.200	0.200	Multipaths at OP
$u_{b,14}$	0.200	0.200	0.200	0.200	Multipaths at visited site
Link of the traveling system to local time scale					
$u_{b,21}$	0.220	0.220		0.220	REFDLY at OP
$u_{b,22}$	0.220	0.220		0.220	REFDLY at visited site
$u_{b,TOT}$	0.626	0.588	0.407	0.694	
Link of the reference system to UTC(OP)					
$u_{b,31}$	0.220	0.220		0.220	REFDLY at OP
Link of the visited system to its local time scale					
$u_{b,32}$	0.220	0.220		0.220	REFDLY at visited site
Antenna cable delays					
$u_{b,41}$	0.000	0.000		0.000	CABDLY at OP
$u_{b,42}$	0.000	0.000		0.000	CABDLY at visited site
Type B uncertainties					
$u_{b,SYS}$	0.700	0.666		0.761	Quadratic sum of u_b
Combined uncertainties					
u_{CAL0}	0.702	0.669		0.777	Composed of u_a and $u_{b,SYS}$

Table 8: **CH04** uncertainty budget for **Galileo** calibrated delays

Uncertainty type	E1	E5a	E1-E5a	E3	Description
u_a(Reference)	0.027	0.049	0.056	0.067	Largest TDEV(1 d) sigma between the start and the end of OP72 or OP74 against OP73
u_a(CH04)	0.027	0.043	0.051	0.069	Largest TDEV(1 d) sigma of offset between visited station and OP72 or OP74
Type A uncertainties					
u_a	0.039	0.065	0.076	0.097	Visited against reference
Misclosure					
$u_{b,1}$	0.361	0.339	0.022	0.389	Actual misclosure offset
Systematic components related to RAWDIF					
$u_{b,11}$	0.200	0.200	0.200	0.200	Position error at OP
$u_{b,12}$	0.200	0.200	0.200	0.200	Position error at visited site
$u_{b,13}$	0.200	0.200	0.200	0.200	Multipaths at OP
$u_{b,14}$	0.200	0.200	0.200	0.200	Multipaths at visited site
Link of the traveling system to local time scale					
$u_{b,21}$	0.220	0.220		0.220	REFDLY at OP
$u_{b,22}$	0.220	0.220		0.220	REFDLY at visited site
$u_{b,TOT}$	0.623	0.610	0.401	0.639	
Link of the reference system to UTC(OP)					
$u_{b,31}$	0.220	0.220		0.220	REFDLY at OP
Link of the visited system to its local time scale					
$u_{b,32}$	0.220	0.220		0.220	REFDLY at visited site
Antenna cable delays					
$u_{b,41}$	0.000	0.000		0.000	CABDLY at OP
$u_{b,42}$	0.000	0.000		0.000	CABDLY at visited site
Type B uncertainties					
$u_{b,SYS}$	0.697	0.685		0.711	Quadratic sum of u_b
Combined uncertainties					
u_{CAL0}	0.699	0.689		0.718	Composed of u_a and $u_{b,SYS}$

Table 9: **CH05** uncertainty budget for **Galileo** calibrated delays

Uncertainty type	E1	E5a	E1-E5a	E3	Description
u_a(Reference)	0.027	0.049	0.056	0.067	Largest TDEV(1 d) sigma between the start and the end of OP72 or OP74 against OP73
u_a(CH05)	0.041	0.044	0.061	0.106	Largest TDEV(1 d) sigma of offset between visited station and OP72 or OP74
Type A uncertainties					
u_a	0.050	0.066	0.083	0.126	Visited against reference
Misclosure					
$u_{b,1}$	0.361	0.339	0.022	0.389	Actual misclosure offset
Systematic components related to RAWDIF					
$u_{b,11}$	0.200	0.200	0.200	0.200	Position error at OP
$u_{b,12}$	0.200	0.200	0.200	0.200	Position error at visited site
$u_{b,13}$	0.200	0.200	0.200	0.200	Multipaths at OP
$u_{b,14}$	0.200	0.200	0.200	0.200	Multipaths at visited site
Link of the traveling system to local time scale					
$u_{b,21}$	0.220	0.220		0.220	REFDLY at OP
$u_{b,22}$	0.220	0.220		0.220	REFDLY at visited site
$u_{b,TOT}$	0.623	0.610	0.401	0.639	
Link of the reference system to UTC(OP)					
$u_{b,31}$	0.220	0.220		0.220	REFDLY at OP
Link of the visited system to its local time scale					
$u_{b,32}$	0.220	0.220		0.220	REFDLY at visited site
Antenna cable delays					
$u_{b,41}$	0.000	0.000		0.000	CABDLY at OP
$u_{b,42}$	0.000	0.000		0.000	CABDLY at visited site
Type B uncertainties					
$u_{b,SYS}$	0.697	0.685		0.711	Quadratic sum of u_b
Combined uncertainties					
u_{CAL0}	0.699	0.689		0.723	Composed of u_a and $u_{b,SYS}$

7 Validation of the result.

7.1 Stability of the reference station.

The reference station in OP was based on a Septentrio PolaRx5TR receiver called OP73. Figure 1 is showing a plot which demonstrate the stability of this GNSS station during the calibration campaign. The plot is the daily averaged offset between the TWSDRR technique (Two-Way Satellite Time and Frequency Transfer, with Satre modem emision and Software Defined Radio reception) between OP and PTB, and the GNSS Common View (CV) time transfer using P3 GPS data between OP and PTB, based on OP73 in OP side and on PTBB in PTB side. In both laboratories, the signal source is a UTC(k) time scale: UTC(OP) and UTC(PTB). In this computation, the time scales being cancelled, what remains is only the offset between the two time transfer techniques.

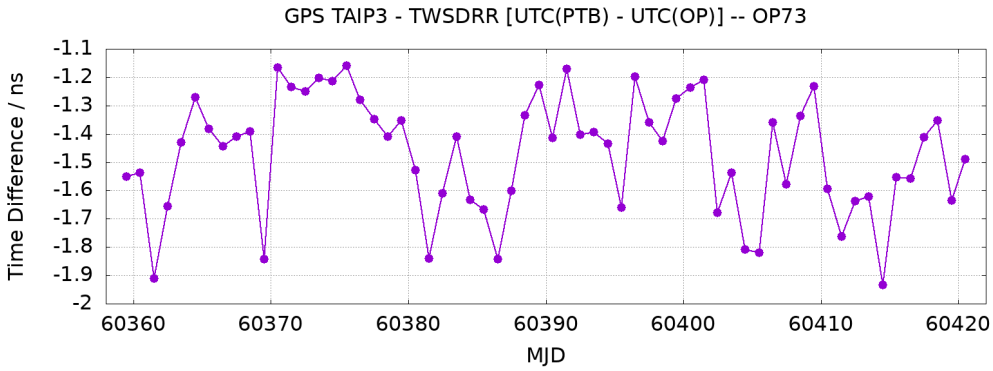

Figure 1: Daily averaged offset between TWSDRR and GPS P3 CV on the link OP-PTB during the calibration campaign.

The mean offset over that period of time is about – 1.5 ns, with a standard deviation of about 0.20 ns. This mean offset is mostly coming from the last G1 calibration of GNSS stations achieved by BIPM for OP and PTB stations (#1001-2022) and from the last TWSTFT relative calibration (#0546-2021). We remind here that the conventional combined uncertainty of GNSS stations located in G1 laboratories is 1.5 ns, as decided by the CCTF Working Group (WG) on GNSS time transfer. The offset seen here is in full agreement with the claimed uncertainties.
What can be seen on Figure 1 is the excellent sub-ns stability of this ensemble of four systems, two inside each laboratory, among which OP73 in OP. This is especially true when considering together the opening and closing periods of the campaign only, MJD 60359–60366 and MJD 60413–60420. We estimate that any potential effect of OP73 on this calibration campaign can be disregarded with respect to the final uncertainty of the calibration.

7.2 Offset between the two traveling receivers.

Figure 2.a is showing the offset between the two traveling receivers during the whole calibration campaign, based on CV between CGGTTS P3 (GPS), and Figure 2.b is showing similar offset based on CV between CGGTTS E3 (Galileo) data, by using for OP72 and OP74 the average delays computed against OP73 between the start and the closure of the campaign. The average offsets between the receivers before, during and after the trip, are lower than 20 ps, with a standard deviation below 100 ps. The traveling equipment remained very stable during the calibration campaign. We can consider that the effect of these offsets on the calibration results is negligible.

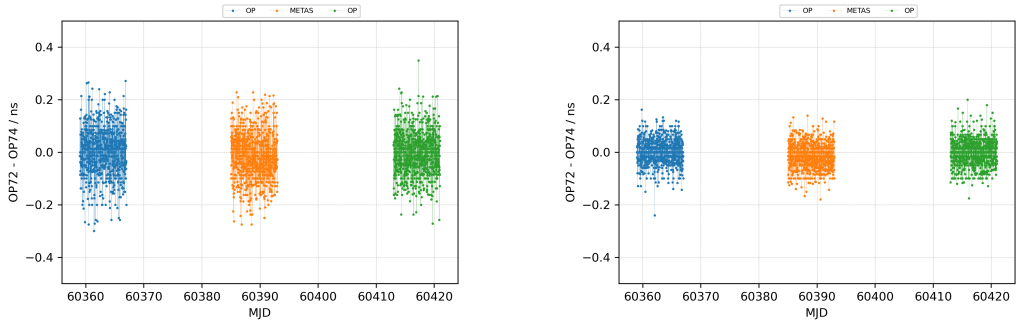

(a) P3 CV

(b) E3 CV

Figure 2: Offset between OP72 and OP74 during the METAS calibration campaign, based on CGGTTS CV data. From left to right, the sequence of data sets is: start at OP, METAS and closure at OP.

7.3 Offset between the two METAS receivers

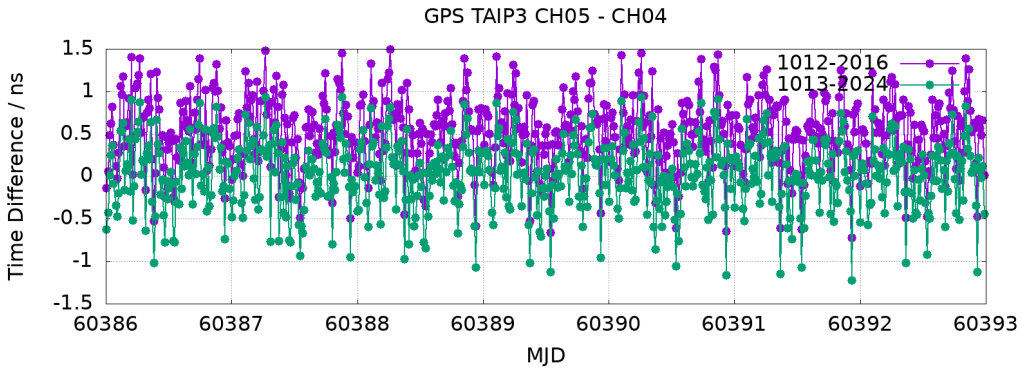

Figure 3: TAIP3 GPS differences between CH04 and CH05.

Figure 3 is showing the offset betwen CH05 and CH04, based on CV between CGGTTS P3 (GPS) using the stations internal delays of the 1012-2016 and 1013-2024 calibration results, respectively. Over the period 60386 - 60393, the average offset is 0.5 ns with a standard deviation below 0.41 ns using the previous calibation delays. With the current calibration, we obtain as expected an average offset of 0.0 ns, with a standard deviation of 0.40 ns.

A Annex A: BIPM information sheet.

A.1 Implementation in OP.

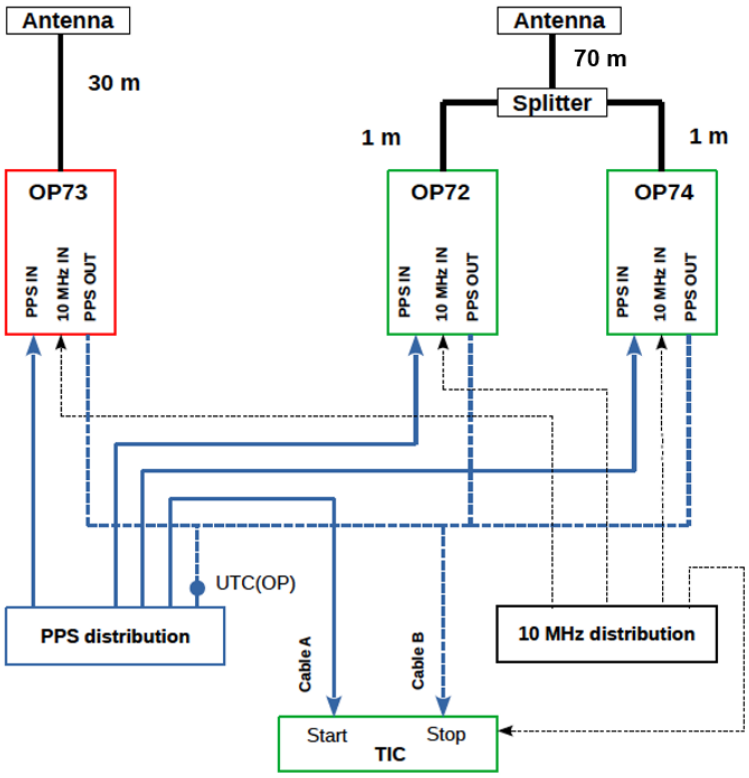

Figure 4: Implementation of OP traveling equipment in OP

A.2 Implementation in METAS.

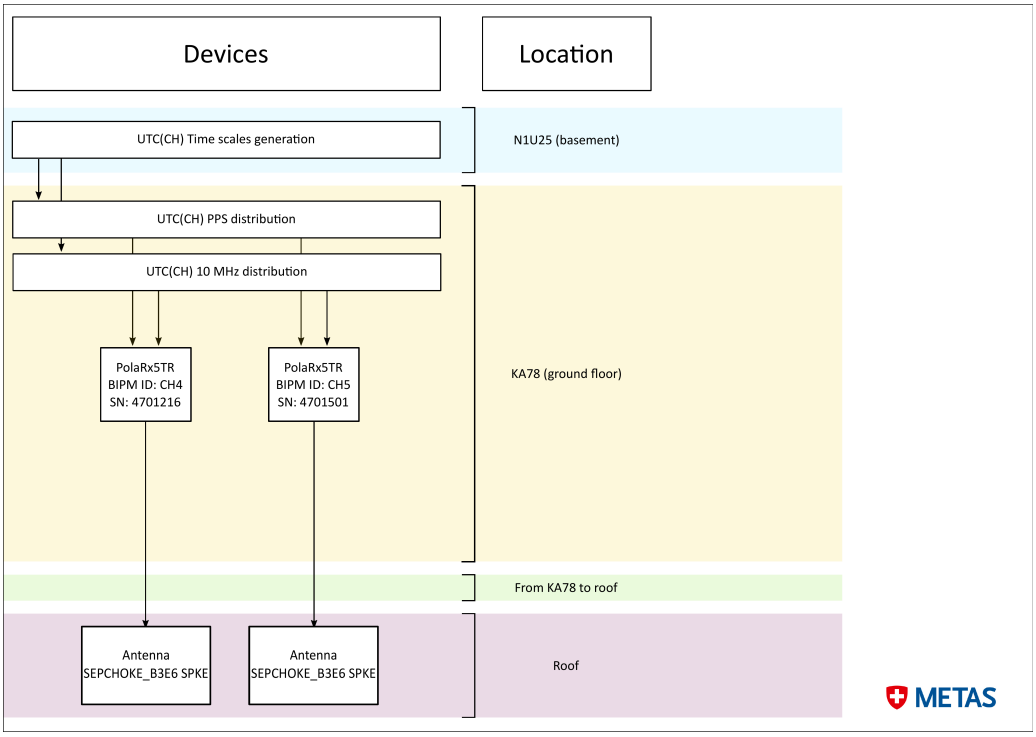

Figure 5: Implementation of METAS equipment

Cal Id: 1013-2024 Version / Date: 11/06/2024

BIPM Information sheet

Laboratory	OP (Open)
Date and hour beginning of measurements	19/02/2024 00:00:00
Date and hour end measurements	26/02/2024 23:59:59

Information on the system			
	Local	**Traveling**	
4-Character BIPM code	OP73	OP72	OP74
Receiver maker and type	PolaRx5TR	PolaRx5TR	PolaRx5TR
Receiver serial number	4701467	4701463	4701497
1 PPS triger level / V	1	1	1
Antenna cable marker and type		HY 400 UF	HY 400 UF
Phase stabilized cable (Y/N)	N	N	N
Cable length outside building / m	20	20	20
Antenna maker and type	SEPCHOKE_B3E6	TWIVP6000	TWIVP6000
Antenna serial number	5858	33-685000-01-01	33-685000-01-01
Temperature if stabilized / °C			

Mesured delays / ns			
	Local	**Traveling**	
Delay from local UTC(k) to receiver 1 PPS_IN			
Delay from 1 PPS_IN to internal reference (see Annex 1)	Compensation disabled	Compensation disabled	Compensation disabled
Antenna cable delay			
Splitter delay			
Additional cable delay			

Data used for the generation of CGGTTS files			
	Local	**Traveling**	
INT DLY (GPS) / ns	P1: 29.55 P2: 26.02	P1: P2:	P1: P2:
INT DLY (Galileo) / ns	E1: 31.78 E5a: 31.52	E1: E5a:	E1: E5a:
CAB DLY / ns	129.6	0.0	0.0
REF DLY / ns	85.2	93.4	111.4
Coordinate reference frame	ITRF	ITRF	ITRF
Latitude or X / m	4202777.071	4202781.410	4202781.410
Longitude or Y / m	171367.028	171369.367	171369.367
Height or Z / m	4778661.392	4778659.061	4778659.061

General Information	
Rise time of local UTC pulse	500 ps
Air conditioning (Y/N)	Y
Set temperature value and uncertainty	22+/-1°C
Set humidity value and uncertainty	NA

Cal Id: 1013-2024 Version / Date: 11/06/2024

BIPM Information sheet

Laboratory	OP (Close)
Date and hour beginning of measurements	13/04/2024 00:00:00
Date and hour end measurements	20/04/2024 23:59:59

Information on the system			
	Local	**Traveling**	
4-Character BIPM code	OP73	OP72	OP74
Receiver maker and type	PolaRx5TR	PolaRx5TR	PolaRx5TR
Receiver serial number	4701467	4701463	4701497
1 PPS triger level / V	1	1	1
Antenna cable marker and type		HY 400 UF	HY 400 UF
Phase stabilized cable (Y/N)	N	N	N
Cable length outside building / m	20	20	20
Antenna maker and type	SEPCHOKE_B3E6	TWIVP6000	TWIVP6000
Antenna serial number	5858	33-685000-01-01	33-685000-01-01
Temperature if stabilized / °C			

Mesured delays / ns			
	Local	**Traveling**	
Delay from local UTC(k) to receiver 1 PPS_IN			
Delay from 1 PPS_IN to internal reference (see Annex 1)	Compensation disabled	Compensation disabled	Compensation disabled
Antenna cable delay			
Splitter delay			
Additional cable delay			

Data used for the generation of CGGTTS files			
	Local	**Traveling**	
INT DLY (GPS) / ns	P1: 29.55 P2: 26.02	P1: P2:	P1: P2:
INT DLY (Galileo) / ns	E1: 31.78 E5a: 31.52	E1: E5a:	E1: E5a:
CAB DLY / ns	129.6	0.0	0.0
REF DLY / ns	85.2	93.3	111.3
Coordinate reference frame	ITRF	ITRF	ITRF
Latitude or X / m	4202777.071	4202781.377	4202781.377
Longitude or Y / m	171367.028	171369.355	171369.355
Height or Z / m	4778661.392	4778659.037	4778659.037

General Information	
Rise time of local UTC pulse	500 ps
Air conditioning (Y/N)	Y
Set temperature value and uncertainty	22+/-1°C
Set humidity value and uncertainty	NA

Cal Id: 1013-2024 Version / Date: 11/06/2024

BIPM Information sheet

Laboratory	METAS
Date and hour beginning of measurements	16/03/2024 00:00:00
Date and hour end measurements	23/03/2024 23:59:59

Information on the system			
	Local	**Traveling**	
4-Character BIPM code	CH04	OP72	OP74
Receiver maker and type	PolaRx5TR	PolaRx5TR	PolaRx5TR
Receiver serial number	4701216	4701463	4701497
1 PPS triger level / V	1	1	1
Antenna cable marker and type	type N	HY 400 UF	HY 400 UF
Phase stabilized cable (Y/N)	N	N	N
Cable length outside building / m	10		
Antenna maker and type	SEPCHOKE_B3E6 SP	TWIVP6000	TWIVP6000
Antenna serial number	5168	33-685000-01-01	33-685000-01-01
Temperature if stabilized / °C			

Mesured delays / ns			
	Local	**Traveling**	
Delay from local UTC(k) to receiver 1 PPS_IN	2.5		
Delay from 1 PPS_IN to internal reference (see Annex 1)	Compensation enabled	Compensation disabled	Compensation disabled
Antenna cable delay	208.9		
Splitter delay			
Additional cable delay			

Data used for the generation of CGGTTS files			
	Local	**Traveling**	
INT DLY (GPS) / ns	P1: 28.2 P2: 25.5	P1: P2:	P1: P2:
INT DLY (Galileo) / ns	E1: E5a:	E1: E5a:	E1: E5a:
CAB DLY / ns	208.9	0.0	0.0
REF DLY / ns	2.6	45.2	63.8
Coordinate reference frame	ITRF	ITRF	ITRF
Latitude or X / m	4327319.1900	4327320.845	4327320.845
Longitude or Y / m	566956.0900	566957.043	566957.043
Height or Z / m	4636427.0000	4636425.530	4636425.530

General Information	
Rise time of local UTC pulse	500 ps
Air conditioning (Y/N)	Y
Set temperature value and uncertainty	22.57+/-0.01
Set humidity value and uncertainty	38.17+/-0.08

Cal Id: 1013-2024 Version / Date: 11/06/2024

BIPM Information sheet

Laboratory	METAS
Date and hour beginning of measurements	16/03/2024 00:00:00
Date and hour end measurements	23/03/2024 23:59:59

Information on the system			
	Local	**Traveling**	
4-Character BIPM code	CH05		
Receiver maker and type	PolaRx5TR		
Receiver serial number	4701501		
1 PPS triger level / V	1		
Antenna cable marker and type	type N		
Phase stabilized cable (Y/N)	N		
Cable length outside building / m	10		
Antenna maker and type	SEPCHOKE_B3E6 SP		
Antenna serial number	5858		
Temperature if stabilized / °C			

Mesured delays / ns			
	Local	**Traveling**	
Delay from local UTC(k) to receiver 1 PPS_IN	9.2		
Delay from 1 PPS_IN to internal reference (see Annex 1)	Compensation Enabled		
Antenna cable delay	220.0		
Splitter delay			
Additional cable delay			

Data used for the generation of CGGTTS files			
	Local	**Traveling**	
INT DLY (GPS) / ns	P1: 25.7 P2: 24.4	P1: P2:	P1: P2:
INT DLY (Galileo) / ns	E1: E5a:	E1: E5a:	E1: E5a:
CAB DLY / ns	220.0		
REF DLY / ns	9.2		
Coordinate reference frame	ITRF		
Latitude or X / m	4327318.3150		
Longitude or Y / m	566952.2230		
Height or Z / m	4636428.2022		

General Information	
Rise time of local UTC pulse	500 ps
Air conditioning (Y/N)	Y
Set temperature value and uncertainty	22.57+/-0.01
Set humidity value and uncertainty	38.17+/-0.08

B Annex B: Plots of raw data and TDEV analysis for GPS and GALILEO.

B.1 GPS calibration.

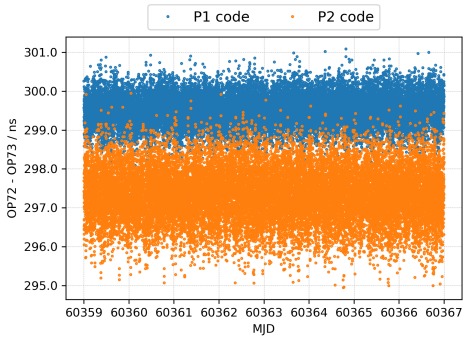

(a) P-code phase differences

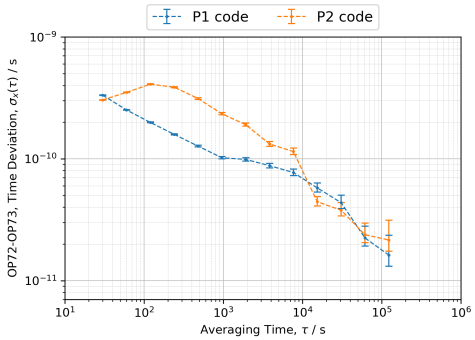

(b) TDEV of P-code delays

Figure 6: Relative calibration of OP72 with respect to OP73 before the trip

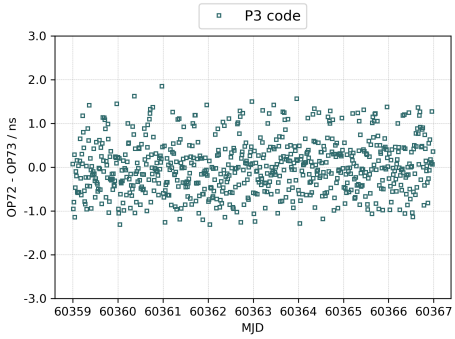

(a) P3 CV after calibration

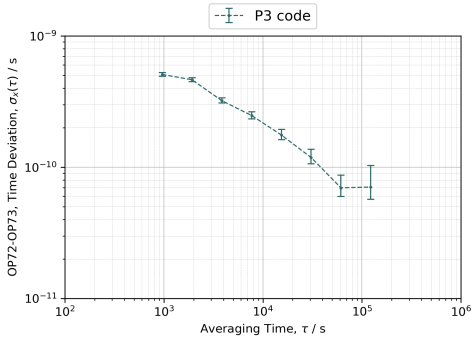

(b) TDEV of P3 CV

Figure 7: P3 CV time difference OP72 with respect to OP73 before the trip

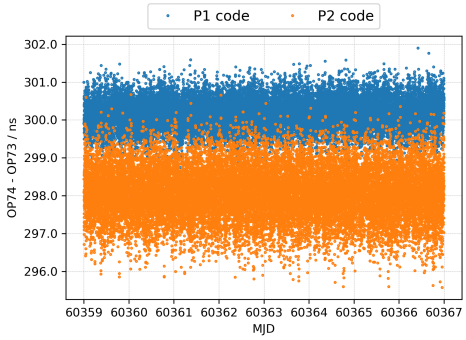

(a) P-code phase differences

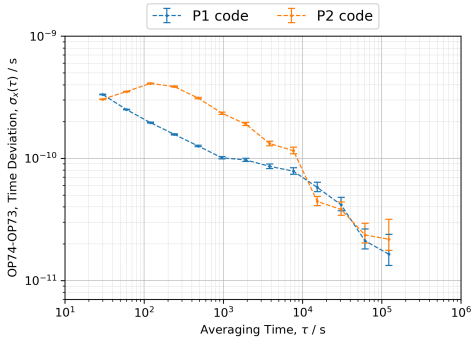

(b) TDEV of P-code delays

Figure 8: Relative calibration of OP74 with respect to OP73 before the trip

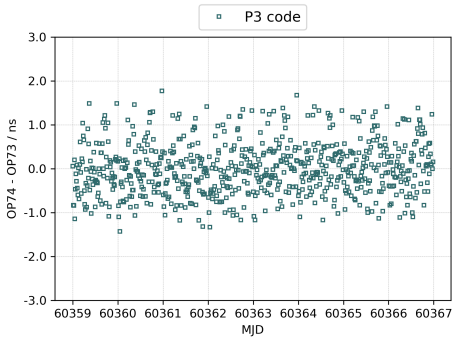

(a) P3 CV after calibration

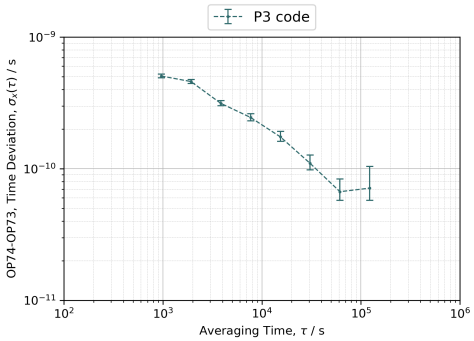

(b) TDEV of P3 CV

Figure 9: P3 CV time difference OP74 with respect to OP73 before the trip

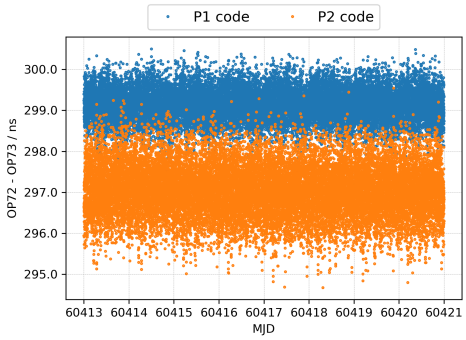

(a) P-code phase differences

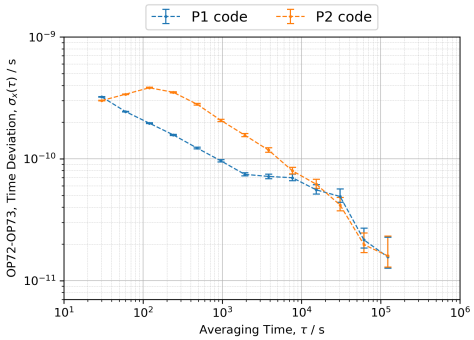

(b) TDEV of P-code delays

Figure 10: Relative calibration of OP72 with respect to OP73 after the trip

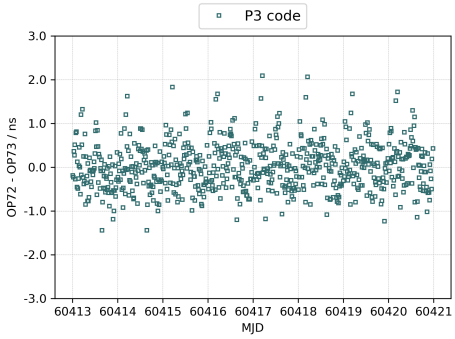

(a) P3 CV after calibration

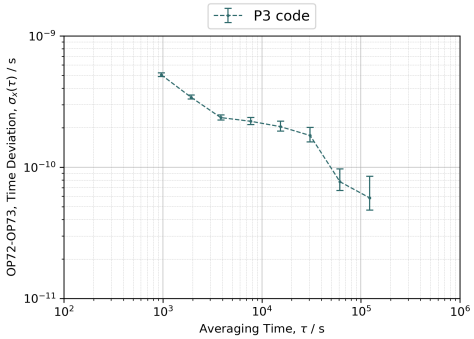

(b) TDEV of P3 CV

Figure 11: P3 CV time difference OP72 with respect to OP73 after the trip

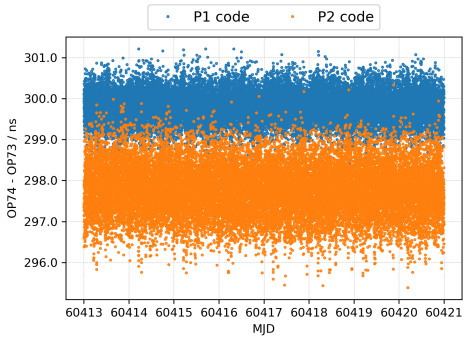

(a) P-code phase differences

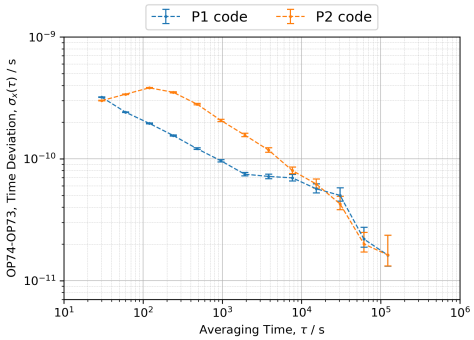

(b) TDEV of P-code delays

Figure 12: Relative calibration of OP74 with respect to OP73 after the trip

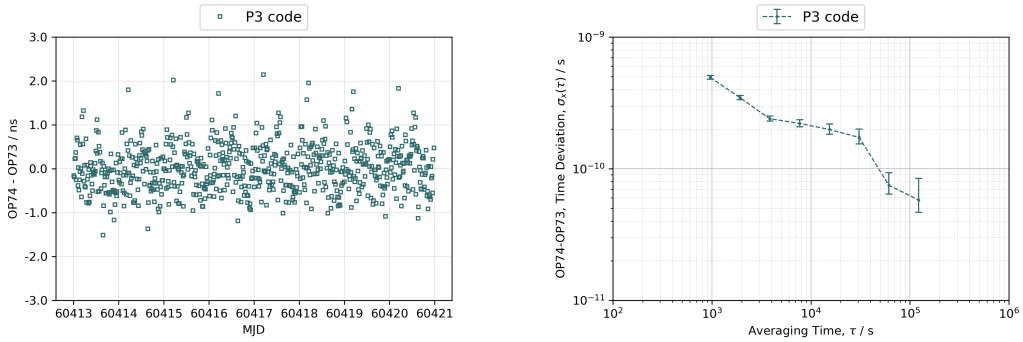

(a) P3 CV after calibration

(b) TDEV of P3 CV

Figure 13: P3 CV time difference OP74 with respect to OP73 after the trip

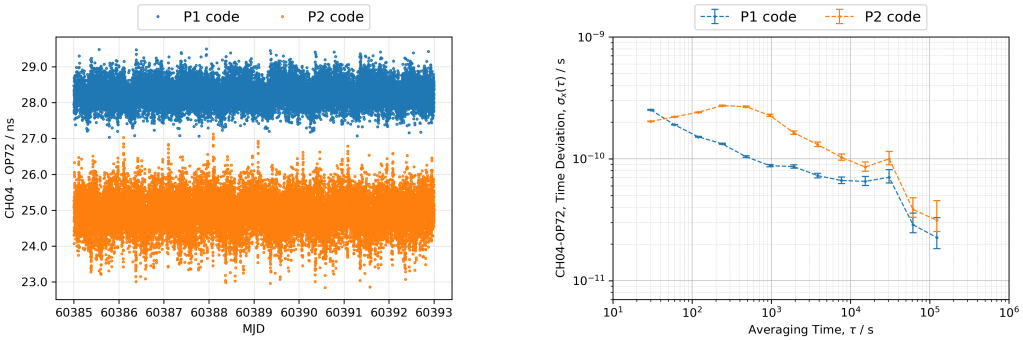

(a) P-code phase differences

(b) TDEV of P-code delays

Figure 14: Relative calibration of CH04 with respect to OP72

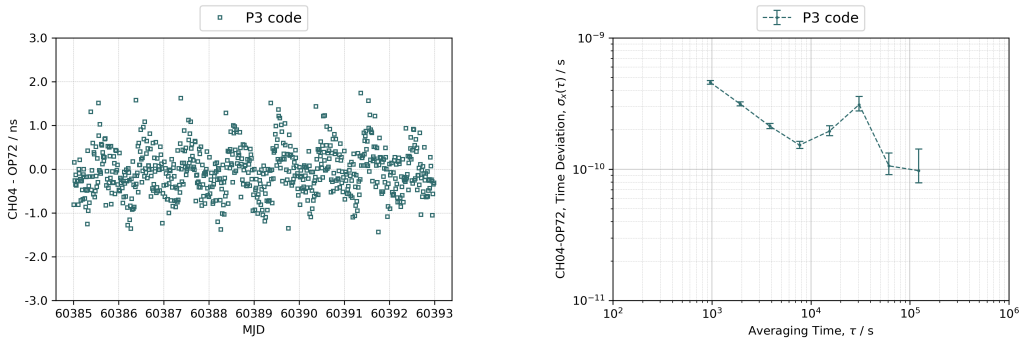

(a) P3 CV after calibration

(b) TDEV of P3 CV

Figure 15: P3 CV time difference CH04 with respect to OP72

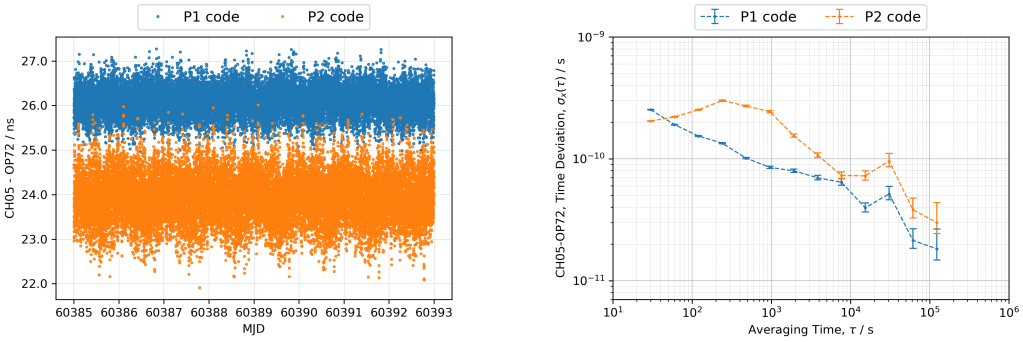

(a) P-code phase differences

(b) TDEV of P-code delays

Figure 16: Relative calibration of CH05 with respect to OP72

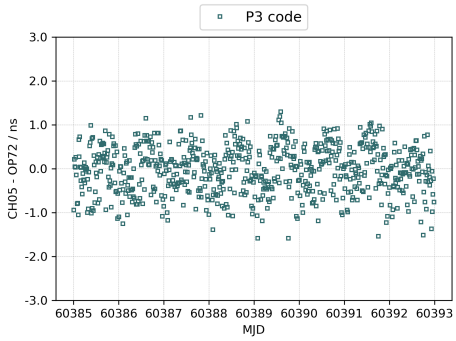

(a) P3 CV after calibration

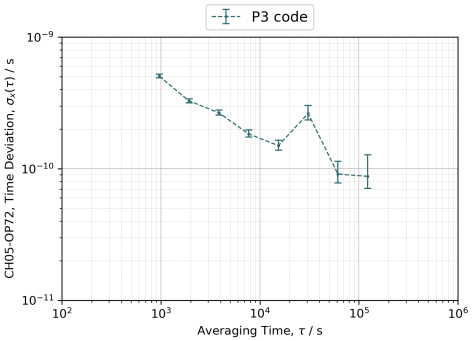

(b) TDEV of P3 CV

Figure 17: P3 CV time difference CH05 with respect to OP72

(a) P-code phase differences

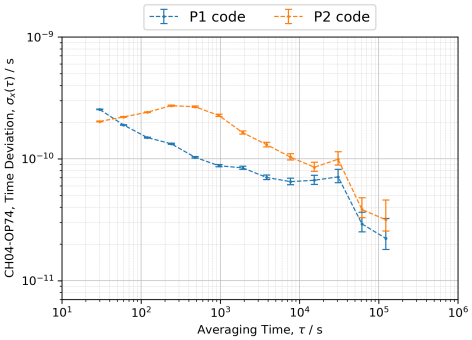

(b) TDEV of P-code delays

Figure 18: Relative calibration of CH04 with respect to OP74

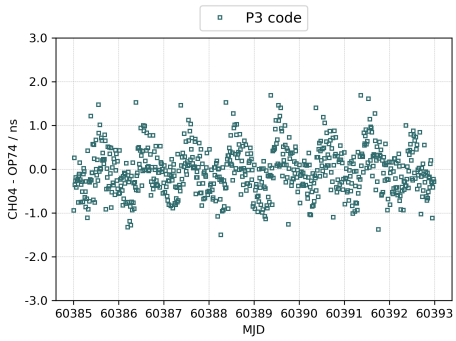

(a) P3 CV after calibration

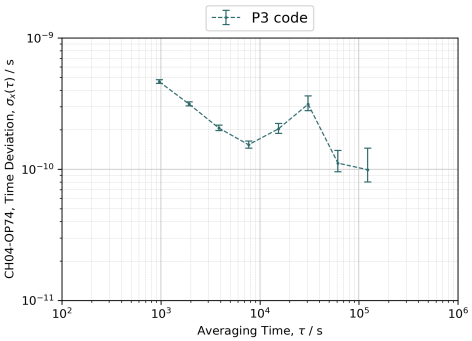

(b) TDEV of P3 CV

Figure 19: P3 CV time difference CH04 with respect to OP74

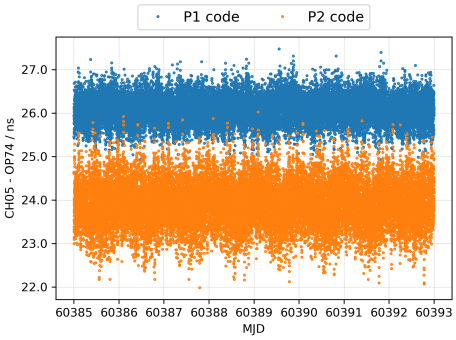

(a) P-code phase differences

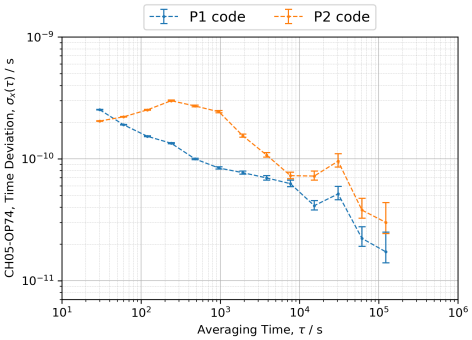

(b) TDEV of P-code delays

Figure 20: Relative calibration of CH05 with respect to OP74

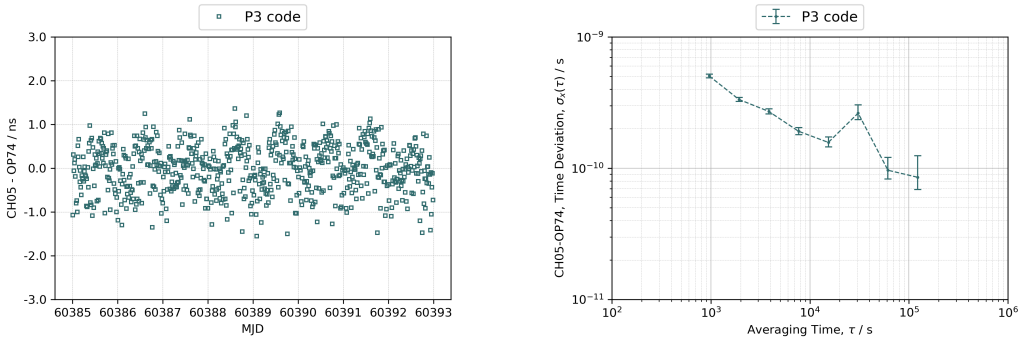

(a) P3 CV after calibration

(b) TDEV of P3 CV

Figure 21: P3 CV time difference CH05 with respect to OP74

B.2 GALILEO calibration.

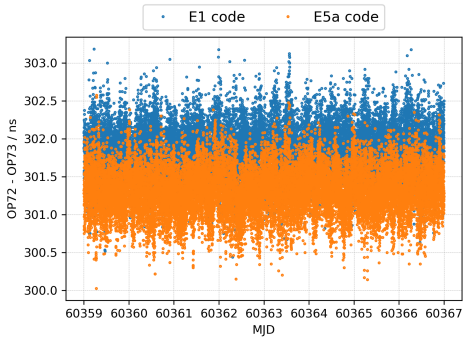

(a) E-code phase differences

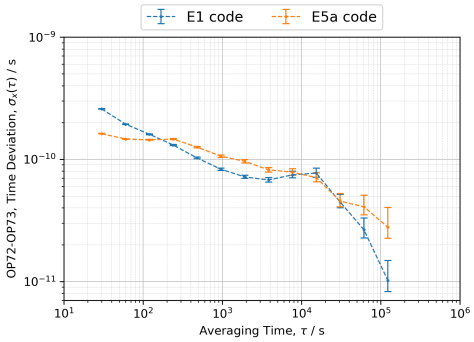

(b) TDEV of E-code delays

Figure 22: Relative calibration of OP72 with respect to OP73 before the trip

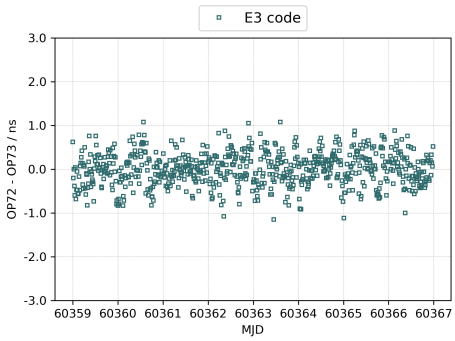

(a) E3 CV after calibration

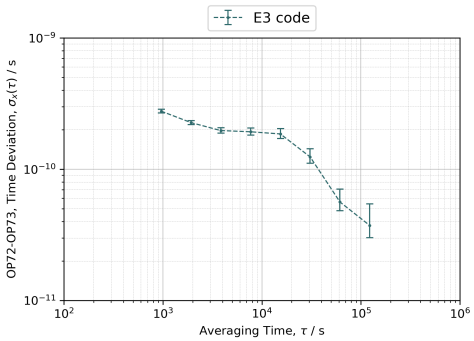

(b) TDEV of E3 CV

Figure 23: E3 CV time difference OP72 with respect to OP73 before the trip

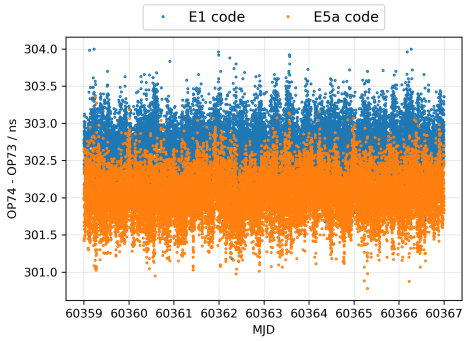

(a) E-code phase differences

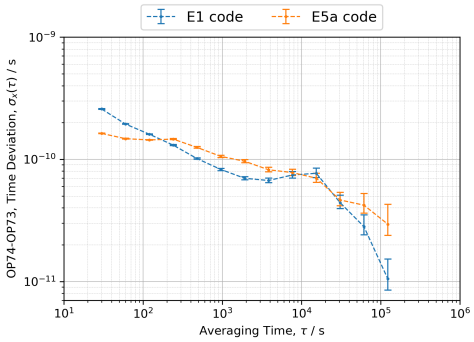

(b) TDEV of E-code delays

Figure 24: Relative calibration of OP74 with respect to OP73 before the trip

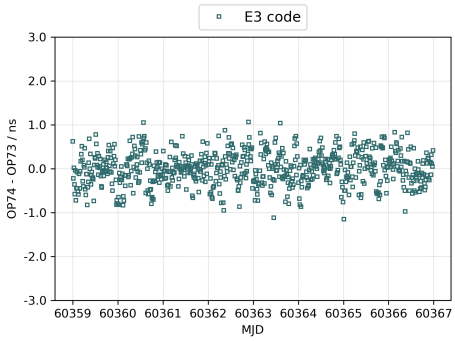

(a) E3 CV after calibration

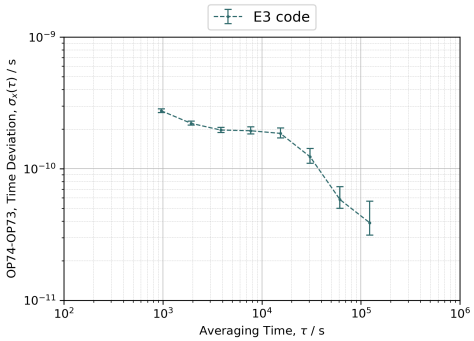

(b) TDEV of E3 CV

Figure 25: E3 CV time difference OP74 with respect to OP73 before the trip

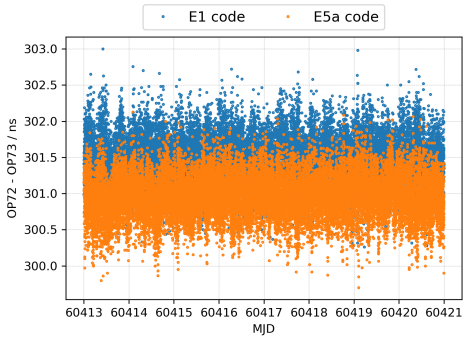

(a) E-code phase differences

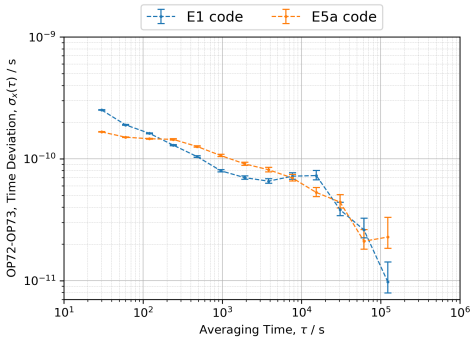

(b) TDEV of E-code delays

Figure 26: Relative calibration of OP72 with respect to OP73 after the trip

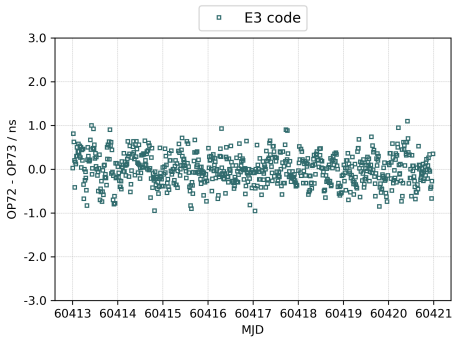

(a) E3 CV after calibration

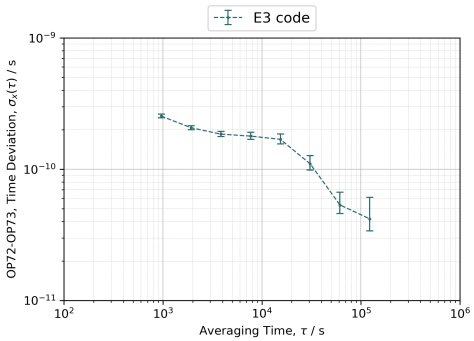

(b) TDEV of E3 CV

Figure 27: E3 CV time difference OP72 with respect to OP73 after the trip

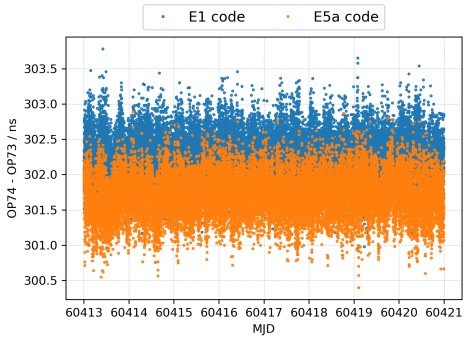

(a) E-code phase differences

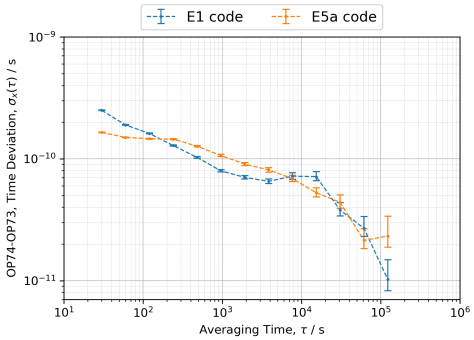

(b) TDEV of E-code delays

Figure 28: Relative calibration of OP74 with respect to OP73 after the trip

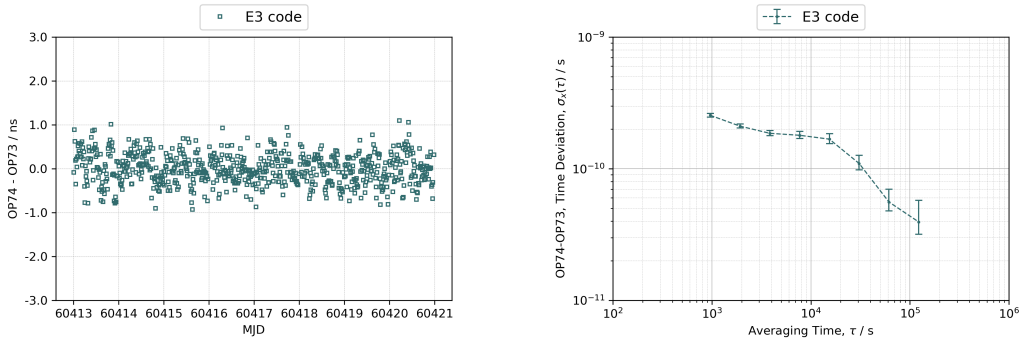

(a) E3 CV after calibration

(b) TDEV of E3 CV

Figure 29: E3 CV time difference OP74 with respect to OP73 after the trip

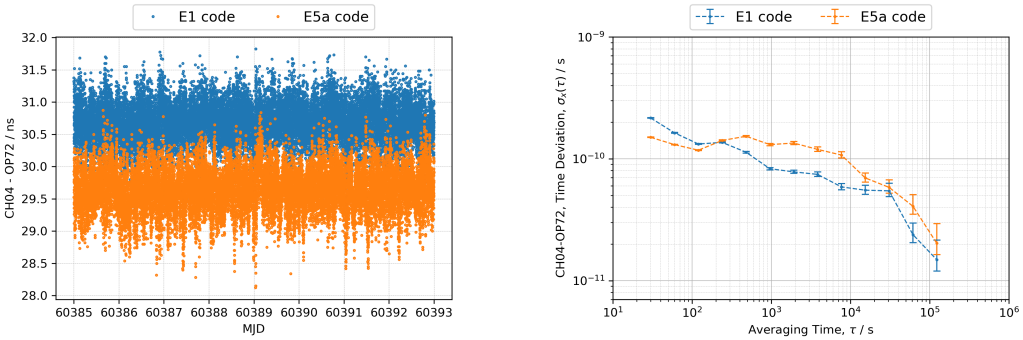

(a) E-code phase differences

(b) TDEV of E-code delays

Figure 30: Relative calibration of CH04 with respect to OP72

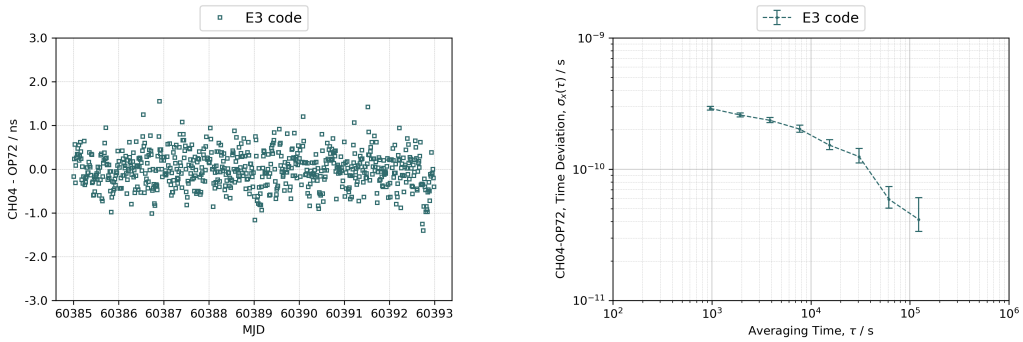

(a) E3 CV after calibration

(b) TDEV of E3 CV

Figure 31: E3 CV time difference CH04 with respect to OP72

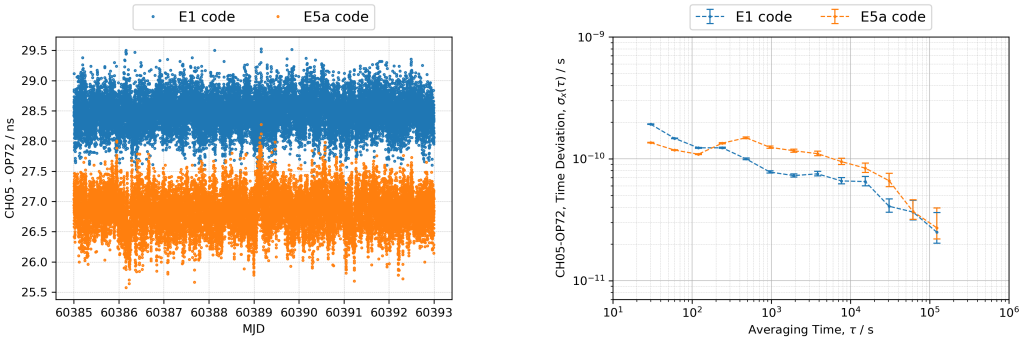

(a) E-code phase differences

(b) TDEV of E-code delays

Figure 32: Relative calibration of CH05 with respect to OP72

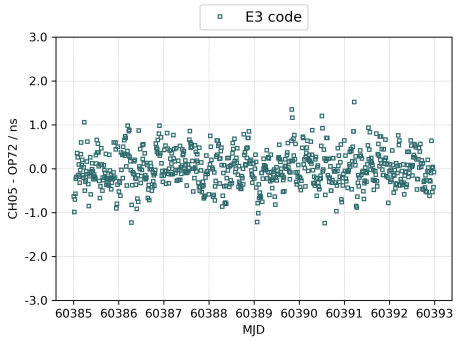

(a) E3 CV after calibration

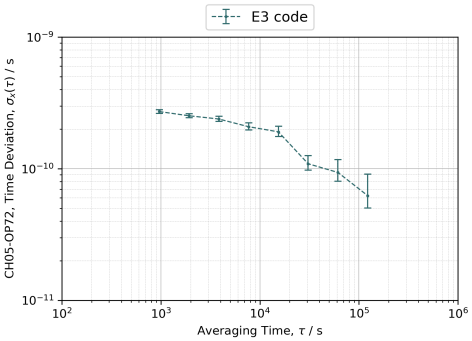

(b) TDEV of E3 CV

Figure 33: E3 CV time difference CH05 with respect to OP72

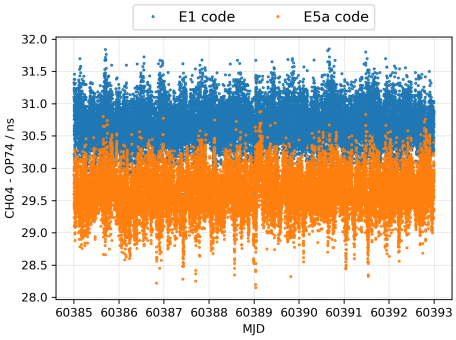

(a) E-code phase differences

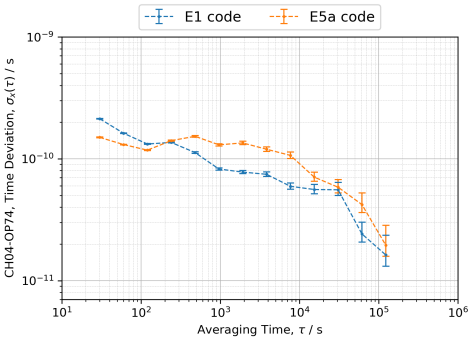

(b) TDEV of E-code delays

Figure 34: Relative calibration of CH04 with respect to OP74

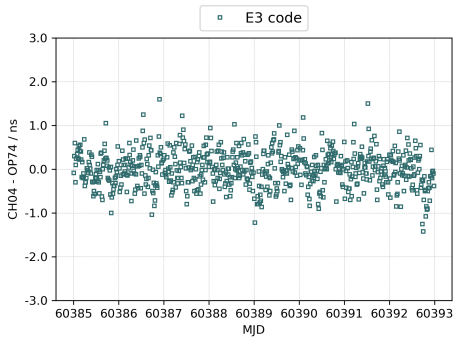

(a) E3 CV after calibration

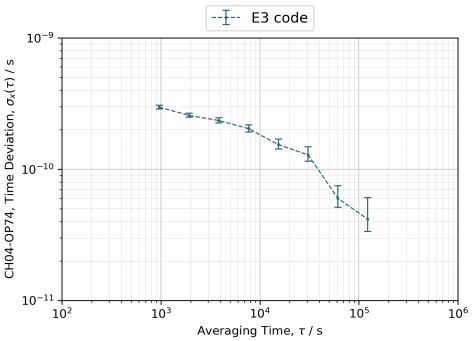

(b) TDEV of E3 CV

Figure 35: E3 CV time difference CH04 with respect to OP74

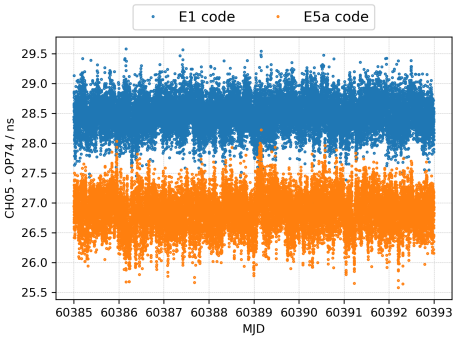

(a) E-code phase differences

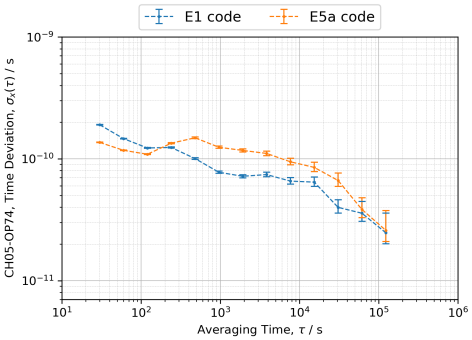

(b) TDEV of E-code delays

Figure 36: Relative calibration of CH05 with respect to OP74

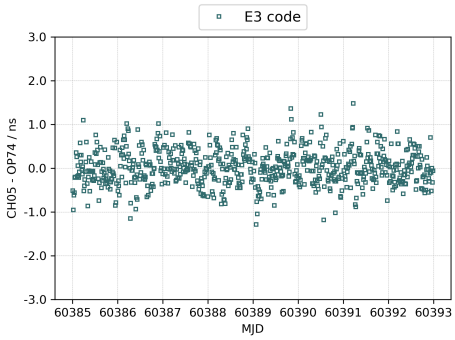

(a) E3 CV after calibration

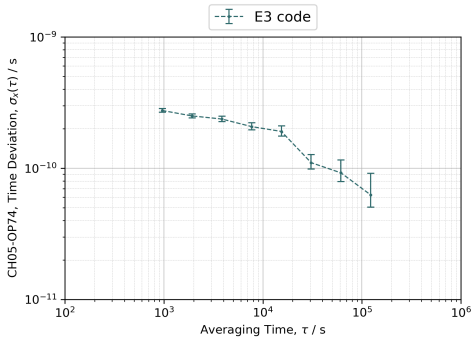

(b) TDEV of E3 CV

Figure 37: E3 CV time difference CH05 with respect to OP74

C Annex C: Uncertainty budget terms.

This section describes the uncertainty budget terms in the case of a calibration with a traveling equipment, including opening and closure measurement at OP.

C.1 Type A uncertainty.

The statistical uncertainty u_a(A-B) for the comparison between two GNSS stations A and B and for each GNSS code is evaluated by computing the upper limit of the error bar of the TDEV at 1 d when possible, or otherwise the upper limit of the last error bar available. The sampling periods of computed calibrated offset usually lead to TDEV data available for 61 440 s and 122 880 s averaging periods. The computed u_a is obtained by a linear interpolation between consecutive TDEV data at an 86 400 s averaging period. When required, a simple quadratic sum leads to the Type A uncertainty required for an uncertainty budget computation.

C.2 Type B uncertainty.

Here are the u_b uncertainties taken into account in the uncertainty budget computations, together with the way they are estimated when necessary.

- $u_{b,1}$ observed maximum misclosure. This uncertainty component is an estimation of the stability of the traveling equipment during the campaign. The misclosure $u_{b,1}$ we used here is the actual misclosure between the start and the end of the campaign.
- $u_{b,11}$ position error at reference site. The position of the center of phase of traveling antenna is estimated at opening and closure by using the NRCan PPP software, while for the OP reference station antenna the coordinates of the last G1 calibration are used. Note that this computation is achieved by using GPS data only. This might lead to a small bias on the phase center of the antenna for Galileo signals. We safely choose a conventional value of 200 ps ($\sim$ 6 cm) for the position error at the reference site.
- $u_{b,12}$ position error at visited site. At visited sites the position of the center of phase of all antennas is estimated by using the NRCan PPP software. Note that this computation is achieved by using GPS data only. This might lead to a small bias on the phase center of the antenna for Galileo signals. We safely choose a conventional value of 200 ps ($\sim$ 6 cm) for the position error at all visited sites.
- $u_{b,13}$ multipath at reference site. We assume in all cases a conventional value of 200 ps, which is in line with some experiment achieved at OP and ORB, especially when using the calibration software developed at OP, where outliers are properly averaged out. (see [2]).
- $u_{b,14}$ multipath at visited site. Same as above.
- $u_{b,21}$ REFDLY (traveling receiver at reference lab). Uncertainty of the measure of the time difference between the reference point of the traveling receiver and the local timescale. The used value is the quadratic sum of an uncertainty value attributed to the Time Interval Counter (TIC) with the standard deviation of the actual measurement (see [3]). When the REFDLY is obtained by summing several individual measurement the uncertainty is increased by quadratic sum as required. We use 220 ps as conservative conventional value.
- $u_{b,22}$ REFDLY (traveling receiver at visited lab). Same as above. This is possible because the TIC we are using for all REFDLY measurements is traveling along with the OP GNSS stations.
- $u_{b,TOT}$: Quadratic sum of all previous u_b.
- $u_{b,31}$ REFDLY uncertainty of the GNSS reference station to its local timescale. Computed similarly as $u_{b,21}$. This term can be set to 0 when the GNSS reference station has been recently calibrated, the uncertainty of REFDLY being already included in the conventional uncertainty decided by the CCTF WG on GNSS.
- $u_{b,32}$ REFDLY uncertainty (at visited lab) of the link of the visited station to its local UTC(k). Computed similarly as $u_{b,21}$. When this delay is measured and the $u_{b,32}$ is taken into account, the local distribution system can be modified afterwards without loosing the calibration of the local GNSS station, provided the new REFDLY is taken into account afterwards
- $u_{b,41}$ uncertainty of the antenna cable delay at reference station. The chosen value here is based on a comprehensive study which is available in reference [4].

- $u_{b,42}$ uncertainty of antenna cable delay at visited station. Same as just above. When for some reason the antenna cable of the traveling system is changed during the campaign, $u_{b,42}$ is typically obtained from the quadratic sum of the uncertainty of the antenna cable delay actually used at the visited station and the uncertainty of the antenna cable delay of the traveling equipment.

- $u_{b,SYS}$: Quadratic sum of all type B uncertainties above.

C.3 Combined uncertainty.

- u_{CAL0}: Quadratic sum of u_a and $u_{b,SYS}$. This uncertainty is for the link between the calibrated station and the reference station, without taking into account the uncertainty of this reference station. Note finally that, in our computation, P3 uncertainty values are not based on a linear combination of P1 and P2 uncertainty values but estimated in a similar way as for P1 and P2. And this is also the case for E3 uncertainty values, which are computed in a similar way as E1 and E5a uncertainty values.